NE

68-FM-299

NATIONAL AERONAUTICS AND SPACE ADMINISTRATION

MSC INTERNAL NOTE NO. 68-FM-299

December 18, 1968

APOLLO 6 ENTRY POSTFLIGHT ANALYSIS

Landing Analysis Branch

MISSION PLANNING AND ANALYSIS DIVISION
MANNED SPACECRAFT CENTER
HOUSTON, TEXAS

MSC INTERNAL NOTE NO. 68-FM-299

PROJECT APOLLO

APOLLO 6 ENTRY POSTFLIGHT ANALYSIS

By Lamar Bolling
Guided Entry Systems Section

December 18, 1968

MISSION PLANNING AND ANALYSIS DIVISION
NATIONAL AERONAUTICS AND SPACE ADMINISTRATION
MANNED SPACECRAFT CENTER
HOUSTON, TEXAS

MSC Task Monitor: John K. Burton

Approved: _____
Floyd Bennett, Chief
Landing Analysis Branch

Approved: _____
John P. Mayer, Chief
Mission Planning and Analysis Division

CONTENTS

TABLES

FIGURES

NOMENCLATURE

AGC	Apollo Guidance Computer
AO	AGC computed pullout drag level
ARS	Apollo reentry simulation
BET	best estimate trajectory
CDU	coupling data unit
CDUX	coupling data unit for the roll axis
c. g.	center of gravity
CM	command module
CSM	command service module
C_D	aerodynamic drag coefficient
C_L	aerodynamic lift coefficient
GAMMAL	AGC computed flight-path angle for atmospheric exit
DIFF	AGC computed difference between the actual range to target and the predicted range to target
g. e. t.	ground elapsed time
G&N	guidance and navigation system
IMU	inertial measurement unit
L/D	aerodynamic lift-to-drag ratio
n mi	nautical mile
PIPA	pulse-integrating pendulous accelerometer
Q7	AGC computed minimum drag level for the Upcontrol phase
RDOT	radial velocity
SPS	service propulsion system
TM	telemetry data recorded by the AGC
VL	AGC computed velocity for minimum drag level (Q7)
V1	AGC computed velocity for pullout

APOLLO 6 ENTRY POSTFLIGHT ANALYSIS

By Lamar Bolling

Guided Entry Systems Section

TRW Systems Group

1. SUMMARY

Postflight evaluation of the operation of the entry Apollo Guidance Computer (AGC) indicates that the computer performed properly throughout the entry phase. The primary evaluation was by comparison of parameters generated by a guidance computer simulation with those parameters which were recorded on telemetry (TM) tape during the flight. Accelerometer data from the TM tape were utilized in the simulation to provide the same data as the onboard computer. This comparison indicates that

- The roll commands are equivalent,
- The time sequence of the guidance logic phases is the same, and
- The state vectors deviate slightly with increasing time, which indicates an accumulation of errors.

The onboard AGC computed position at the time of touchdown was $157^{\circ}49'$ W and $27^{\circ}30'$ N. The simulated AGC position at touchdown was $157^{\circ}48'$ W and $27^{\circ}28'$ N.

The Apollo 6 command module (CM) reached the entry interface in an area of the entry corridor where a known guidance software problem existed. For this area, the initial reference trajectory computed was unobtainable, so the computer iterated to get a suitable reference trajectory. In this iteration, one of the variables, the acceleration at atmospheric exit, was not programmed for recomputation after the initial pass through the prediction logic. The failure to recompute the acceleration at atmospheric exit depressed the actual trajectory prior to atmospheric exit and resulted in a touchdown point short of the target. The actual target miss distance was less than preflight predictions with similar entry conditions resulting from greater than expected CM aerodynamic capabiltiy. The CM pickup point was 49 nautical miles short of the planned touchdown point.

Simulations of the actual environment trajectory were done for two situations which utilized the TM data from the onboard computer. The first simulation, the coupling data unit (CDU) drive trajectory, utilized the desired flight steering commands which were generated by the onboard computer. This trajectory resulted in a touchdown point 38.5 nautical miles from the command module pickup point. The second simulation, the pulse-integrating pendulous accelerometer (PIPA) drive trajectory, computed the roll commands by utilizing the accelerometer data. This trajectory resulted in a touchdown point 22.5 nautical miles from the CM pickup point. Time histories of the velocity, altitude, and load factor for these two simulations closely match the corresponding data from the 21-day best estimate trajectory (BET) reconstruction.

The Apollo reentry simulation (ARS) program was utilized to generate the simulations.

2. INTRODUCTION

2.1 Purpose

The primary purpose of this report is to present an evaluation of the operation of the Apollo 6 entry guidance and navigation (G&N) system. A second purpose is to evaluate the use of the TM tape data in reconstructing the entry trajectory. This work was performed according to the agreement in Reference 1.

2.2 General Description of Contents

The location of the data discussed in this report is presented below. The data are divided into three sections: "Entry Conditions and Input Data", "AGC Operation Evaluation", and "Trajectory Reconstruction".

The section "Entry Conditions and Input Data" presents the entry state vectors, CM aerodynamics, atmosphere model, and CM mass properties used in the postflight evaluations. Entry state vectors for the environment, AGC, and the preflight contingency no second service propulsion system (SPS) burn are included. The CM aerodynamics computed from the PIPA data on the TM tape is presented and compared to the preflight aerodynamics. Selection of the atmosphere model for postflight evaluation is discussed. Postflight mass properties are presented.

"AGC Operation Evaluation" presents the methods and data used in evaluating the AGC. The effects of the known guidance software problem in the flight are discussed. Time of entrance into the different phases of the guidance logic is presented and significant events occurring during the phases are discussed. The data calculated by the Apollo 6 AGC and recorded on the TM tape is discussed and compared to corresponding data from postflight simulations. Dispersions in the touchdown location due to individual inertial measurement unit (IMU) errors are presented. These errors were computed from the determined IMU error for the Apollo 6 and previously generated dispersion data for 3σ IMU errors. The ratio of the determined errors to the 3σ values were used as multiplication factors for the previously determined dispersions.

The section "Trajectory Reconstruction" presents the reconstructed trajectories which were determined by two different types of external steering. Steering commands and input data to the AGC to calculate steering commands were taken from the TM tape. Trajectory parameters from these reconstructions are compared to the 21-day BET.

3. ENTRY CONDITIONS AND INPUT DATA

This section presents the entry state vectors and input data used in the Apollo 6 postflight analysis. An environmental entry state vector from the 21-day BET and an AGC entry state vector from the TM tape were used in the analysis. An environmental entry state vector obtained from tracking data was used in the initial analysis to select an atmosphere model. CM aerodynamics were computed from TM data. The selection of the atmosphere model is discussed. CM postflight mass properties are presented.

3.1 Entry State Vector

The actual Apollo 6 entry state vector was greatly different from the planned entry state vector with an inertial velocity of 36,500 feet per second and an inertial flight-path angle of 6.4979 degrees below the horizontal. The SPS was used for the alternate mission burn because the Saturn S-IVB did not fire and there was not enough SPS fuel left for the second SPS burn. However, the actual entry state vector was similar to the preflight contingency no second SPS burn entry state vector listed in Table I.

Two entry state vectors were used in the analysis; one for the environment and the other for the AGC (Table I). These two entry state vectors reflect the difference between the postflight environment CM state vector and the state vector in the AGC. The time of entry interface for postflight analysis was determined to be a ground elapsed time (g.e.t.) of 9 hours 38 minutes 26.56 seconds. The environment entry state vector from the 21-day BET is listed below:

inertial velocity	32,829.32 ft/sec
inertial flight-path angle	5.863 deg below the local horizontal
inertial azimuth	89.926 deg
longitude	166°14.94' East
geodetic latitude	32°44.04' North
altitude	401,400 ft

The AGC entry state vector taken from the TM tape was as follows:

inertial velocity	32,836.566 ft/sec
inertial flight-path angle	5.8907 deg below the local horizontal
inertial azimuth	89.8636 deg
longitude	166°12.36' East
geodetic latitude	32°43.93' North
altitude	392,512 ft

The initial entry state vector obtained, shortly after the flight, from tracking data was utilized in selecting the atmosphere and in the initial analysis. This vector is listed in Table I.

3.2 Aerodynamic Data

Aerodynamic data for the postflight simulations were determined from data recorded during the flight. Trim aerodynamic lift-to-drag (L/D) ratios were computed from PIPA data on the TM tape by the method described in Reference 2. Figure 1 presents a time history of L/D's computed from the raw PIPA data. The final aerodynamic coefficients used in the trajectory simulations were derived from the L/D's in Reference 3, which were computed from corrected PIPA data. These L/D's, Figure 2, were converted to lift (C_L) and drag (C_D) coefficients, and the coefficients were used as a function of Mach number. The CM velocity from the BET and the speed of sound from the 1962 U. S. Standard Atmosphere were used in determining the Mach number (Figure 1). For Mach numbers 5.0 and above, the L/D's were converted to lift and drag coefficients from data in Reference 4. The trim angles-of-attack were obtained from Reference 3 and from data in Reference 4. For Mach number below 5.0, the aerodynamic lift and drag coefficients and trim angles-of-attack were computed from the center of gravity (c.g.) locations presented in Section 3.4. Table II lists the lift and drag coefficients, trim angles-of-attack, and L/D's as a function of Mach number which were utilized for postflight simulations. Also listed in the table are the corresponding values which were utilized in the preflight simulations.

A comparison of the preflight and postflight data shows that the CM had more aerodynamic capability than was predicted. Also, the L/D increased as the Mach number decreased until the Mach number reached 5.0. This enabled the CM to land closer to the planned touchdown point than would have been predicted using preflight aerodynamics data.

3.3 Atmosphere Model

The atmosphere model selected for this analysis was the 30° North January atmosphere. With the initial entry state vector from the tracking data, the load factor time history and peak load factor obtained from this atmosphere model matched the corresponding values from the TM tape more closely than any other atmosphere model available. Using the selected atmosphere model, 0.05g was reached 38 seconds after entry, and a peak load factor of 4.61g occurred 100 seconds after entry. Actual flight data indicated that the CM reached 0.05g 40 seconds after entry and reached a peak load factor of 4.66g 100 seconds after entry. This atmosphere model produces heating rates which match those measured onboard the CM, and the atmospheric densities closely match the densities computed from sensed pressure data.

3.4 CM Mass Properties

The CM postflight mass properties presented below are from Reference 5. The CM weight was modified slightly from the preflight value, but the physical dimensions of the vehicle remained the same. The postflight CM weight of 12,512.9 pounds was 5.9 pounds greater than the preflight weight. The c.g. locations in the Apollo coordinate system are listed below in inches:

$$X = 1039.2$$

$$Y = 0.3$$

$$Z = 6.4$$

The moment of inertia about the X-axis was 6554 slug feet squared. Moments of inertia about the Y- and Z-axes and the products of inertia were not used in the four degrees-of-freedom simulations.

4. AGC OPERATION EVALUATION

The methods and data used in evaluating the operation of the Apollo 6 AGC are presented in this section. There existed a known software problem in the guidance system which was encountered during the flight, and the effects of this are discussed. Time of AGC transfer into the guidance phases and significant events occurring during the phases are presented. AGC computed state vector, roll commands, inertial ranges-to-target, and predicted crossrange misses are presented. The IMU errors determined in postflight analysis are used to compute AGC dispersions at touchdown.

The operation of the AGC was evaluated by analysis of the actual AGC flight data and comparisons of these data with postflight simulations. AGC data were recorded on TM tape during the flight and later processed into a form for postflight analysis. In the postflight simulations, the AGC was initialized at the entry interface with the AGC state vector from the TM tape. The PIPA data recorded on the TM tape at 2-second intervals were inputs to the simulated AGC. Except for possible errors in recording or processing the TM data, this provided the simulated AGC with the same initial conditions and the same inputs as the actual AGC. However, the simulations did not reflect interaction of the AGC with other electronic hardware and did not account for timing delays in electronic circuits.

4. 1 Discussion of Guidance Software Problem

For the Apollo 6 mission, there existed a known software problem in the entry G&N logic which occurred for certain areas of the entry corridor when the range-to-target from the entry interface was greater than 1400 nautical miles. The CM entered in this area of the corridor and the relative range-to-target was 1924 nautical miles. Reference 6 gives a description of this problem and the targeting philosophy which was considered during the flight.

The following is a description of the AGC logic in the two phases of the system which were affected by this problem. In the Huntest phase of the guidance logic, a reference trajectory for the remaining flight is computed. The Upcontrol phase controls the CM in order to reach the exit conditions determined in the Huntest phase. On the initial entry, the AGC transfers into the Huntest phase when a radial velocity (RDOT) of -700 feet per second or greater is sensed. The pullout drag level (AO) and the pullout velocity (V1) are predicted. Using AO and V1, the exit velocity (VL) and the exit flight-path angle (GAMMAL) are computed by assuming an exponential atmosphere and a constant L/D. If GAMMAL is negative, the computed exit conditions cannot be achieved, so the minimum drag level for exit (Q7) which is initially 6 feet per second per second is recomputed to a higher value, and GAMMAL is set equal to zero. Based upon the present and computed conditions, ranges for the Huntest, Upcontrol, Kepler, and Final phases are computed and this range compared to the actual range to target. If the absolute value of DIFF (the actual range to target minus the predicted range) is less than 25 nautical miles, a solution has been

reached in the Huntest phase and the AGC transfers into the Upcontrol phase. If DIFF is negative and a solution was not reached in Huntest, the AGC will compute an L/D for constant drag, check the lateral logic, and return to the Huntest phase on the next 2-second cycles. If DIFF is positive, the AGC will remain in the Huntest phase until a solution is reached. V1 will be incremented and a new VL and GAMMAL computed until DIFF is less than 25 nautical miles. However, a new Q7 is not computed when V1 is incremented and herein lies the problem. Since Q7 has a higher value than it would have had if it had been recomputed along with VL and GAMMAL, a non-optimal reference trajectory will be computed. This will depress the trajectory in the Upcontrol phase and reduce the predicted Upcontrol range.

On the actual Apollo 6 flight, the initial GAMMAL was negative and a Q7 of approximately 26 feet per second per second was computed. DIFF was positive so V1 was incremented until DIFF was less than 25 nautical miles. This non-optimal reference trajectory produced 44 seconds of negative lift commands during the Upcontrol phase.

4.2 Guidance Phases

The Apollo 6 G&N logic was divided into five phases: Initial Roll, Huntest, Upcontrol, Kepler and Final phase. In the actual flight, the guidance logic was divided into programs and the program numbers changed each time the AGC changed phases except for the entrance into Huntest. Entrance into Huntest can be determined by a large change in the value of DIFF. The actual AGC and the simulated AGC entered each of the guidance phases at the same time as listed below:

g. e. t. (hr:min:sec)	Phase
9:39:06.56	Initial Roll
9:39:58.56	Huntest and Upcontrol
9:42:18.56	Kepler
9:43:54.56	Final phase

In the actual flight, the roll command at entry interface (9 hours 38 minutes 26.56 seconds) was 15.2 degrees. This roll command of 15.2 degrees resulted from the AGC's effort to reduce the predicted cross-range miss. Both the actual and the simulated AGC's sensed 0.05 g at 9 hours 39 minutes 6.56 seconds and entered the initial roll phase of the guidance logic. One of the main functions of the initial roll phase was to determine if the lift vector should be up or down. The Apollo 6 AGC, as

did the simulated AGC, correctly determined that the lift vector should be up and the roll command remained at 15. 2 degrees.

On the initial plunge, the AGC was programmed to transfer into the Huntest phase when an RDOT of -700 feet per second was sensed. Due to the guidance logic and the existing conditions, the AGC also entered the Upcontrol phase on the same computation cycle. The value of RDOT when the AGC entered Huntest, as computed from TM data, was -650. 3 feet per second and the corresponding value from the simulation was -647. 6 feet per second. The new Q7 computed by the AGC, as determined from TM data, was 26. 3 feet per second per second compared with 26. 1 feet per second per second computed in the simulation. DIFF computed by the actual AGC was -14. 3 nautical miles and -19. 2 nautical miles in the simulation.

In the Upcontrol phase, at a g. e. t. of 9 hours 40 minutes 16. 56 seconds, the first roll command greater than 15. 2 degrees occurs. The actual AGC produced a roll command of 76. 2 degrees and the simulation produced a roll command of 81. 8 degrees. Following these roll commands, both the actual and simulated AGC's commanded negative lift for 44 seconds. These commands for negative lift result from the AGC's operation to satisfy the exit conditions computed in the Huntest phase. A change in sign on the roll command was produced by the lateral logic at a g. e. t. of 9 hours 41 minutes 0. 56 seconds in both AGC's. These commands caused the lift vectors to roll underneath to the opposite side. The reversed roll commands were -90. 4 degrees from the Apollo 6 AGC and -90. 6 degrees from the simulated AGC. The negative lift and the lift vector rolling underneath to the opposite side depressed the range in the Upcontrol phase.

The last roll commands before the Kepler phase were -40. 4 and -40. 3 for the actual AGC and the simulation, respectively. No roll commands were generated during the Kepler phase, so a bank angle close to the last roll command was maintained until the Final phase.

During the Final phase, the lift vector was up, in both the actual flight and the simulation, to compensate for the depressed range in the Upcontrol phase. The roll command was modified from zero to 15. 2 degrees by the lateral logic when the predicted crossrange miss exceeded one-half of the predicted CM lateral maneuverability. Guidance terminated at a g. e. t. of approximately 9 hours 50 minutes 10 seconds when the relative velocity became less than 1000 feet per second. At this time, the AGC state vector was 40. 9 nautical miles from the planned target.

The AGC phases are depicted in Figure 3 which is a plot of the altitude from the BET as a function of the range to the target from the AGC data recorded on the TM tape.

4. 3 AGC Computations

The data computed by the simulated AGC are in very good agreement with the data recorded on the TM tape. Roll commands from the simulated AGC and the TM tape (Figure 4) are almost identical. Table III lists these

roll commands at times when the roll commands are changing. The greatest difference between the roll commands from the two sources occurs during the Final phase. In both cases the lift vector was up in an attempt to compensate for the range lost during the Upcontrol phase. However, the lateral logic section of the guidance logic altered the roll commands of zero by 15.2 degrees in order to reduce the predicted crossrange miss. The Apollo 6 AGC alternately produced sequences of zero- and 15.2-degree roll commands from a g.e.t. of 9 hours 46 minutes 36.56 seconds until 9 hours 48 minutes 38.56 seconds and then kept a 15.2 degree roll command until guidance termination. The simulated AGC held a roll command of 15.2 degrees from a g.e.t. of 9 hours 45 minutes 22.56 seconds until guidance termination.

The inertial velocity, inertial range-to-target, and the predicted crossrange miss from the Apollo 6 AGC and the simulated AGC are presented in Table IV for the times of entry interface, entrance into the guidance phases, and guidance termination. The greatest difference between the two lists occurs in the predicted crossrange miss. This value is calculated from the velocity vector and the target vector and will reflect any differences in these two vectors.

AGC state vectors from the TM tape and from the simulation are presented in Table V for several times during the trajectories. The differences between the components of the state vectors increase with increasing time indicating a timing error, a difference in scaling the PIPA data, or integration. However, the magnitudes of these differences do not indicate unreasonable errors for this length of time.

The Apollo 6 AGC coordinates in the navigation system at drogue deploy transformed into longitude and latitude give 157°49'W and 27°30'N, which is 11.7 nautical miles from the CM pickup point (Figure 5). The simulated AGC touchdown point was 157°48'W and 27°28'N, which is 12.6 nautical miles from the CM pickup point. Figure 5 summarizes the relative positions of the target, pickup, and simulation touchdown points.

The AGC altitude at the time of drogue deploy (9 hours 51 minutes 26.15 seconds) was -14,823 feet. Drogue deploy nominally occurs at an altitude of 23,500 feet so this gives an altitude error of approximately -38,000 feet in the AGC at drogue deploy. This altitude error is less than the 57,000 foot altitude error at drogue deploy in the Apollo AS-501 (CSM-017) computer (Reference 7). The simulated AGC altitude at the time of drogue deploy was 2,681 feet.

4.4 IMU Hardware Errors

Dispersions in the AGC state vector at touchdown due to IMU hardware errors are very small. Accelerometer biases, accelerometer scale factors, and gyro drifts were considered in determining the dispersions, but accelerometer misalignments were not included. These errors as derived under MSC/TRW Task E-38A and reported in Reference 8 are listed below:

X-axis accelerometer bias	-0.190 cm/sec^2
Y-axis accelerometer bias	-0.491 cm/sec^2
Z-axis accelerometer bias	-0.170 cm/sec^2
X-axis accelerometer scale factor	-555 pulses per million
Y-axis accelerometer scale factor	- 75 pulses per million
Z-axis accelerometer scale factor	15 pulses per million
X-axis gyro drift rate	6.0 meru
Y-axis gyro drift rate	-0.8 meru
Z-axis gyro drift rate	-1.6 meru

Determination of hardware errors were hampered by TM data losses just after lift-off and the derived values were not a unique combination, but rather satisfied certain imposed constraints and provided an error model which not only gave good agreement with radar data in the boost phase but also gave satisfactory agreement with the actual splashdown point.

Dispersions resulting from hardware error were computed from data in Reference 9 which present dispersion effects for 3σ errors. The ratios of the determined errors to the 3σ values were used as multiplication factors to determine dispersions at touchdown. IMU errors were considered individually and no combinations of errors were evaluated. Dispersions caused by the IMU errors were computed in a topocentric reference system at touchdown. The positive X-axis was downrange, the positive Z-axis was directed from the center of the earth through the vehicle, and the Y-axis completed the right-hand coordinate system. The X, Y, and Z axes will closely correspond to longitude, latitude, and altitude, respectively for the Apollo 6 flight. Table VI presents the ratios of the IMU errors for Apollo 6 to the 3σ values from Reference 9 and the dispersions resulting from these errors. In order to obtain the actual position, the considered errors would have to be removed from the system. The sign on the presented values would be changed if the errors were removed from the system.

As a result of the method used in determining AGC position vector dispersions at touchdown, a great amount of confidence can not be placed in the specific numbers. However, the small values of these numbers indicate that the IMU errors considered do not account for the differences between the CM pickup point and the AGC longitude and geodetic latitude at drogue deploy. Differences between the AGC and environment state vectors at entry propagate to touchdown and could be a major source for the differences in AGC and environment positions at touchdown.

The longitude and geodetic latitude difference between the environment entry state vector and the AGC entry state vector was 2.2 nautical miles and 0.1 nautical miles, respectively. These differences are in the same direction as the differences between the CM pickup point and the AGC coordinate location at drogue deploy. At entry interface, the altitude for the environmental trajectory was 8,900 feet higher than the altitude of the AGC. At drogue deployment (nominally at an altitude of 23,500 feet) the AGC altitude was -14,823 feet. These differences between the AGC and environment position vectors propagate, and increase, from entry to touchdown.

5. TRAJECTORY RECONSTRUCTION

Reconstructed entry trajectory data are presented in this section. These data are compared to the 21-day BET.

The Apollo 6 entry trajectory was reconstructed in two ways, both using external drives. The first, referred to as a CDU drive, used the CDU data from the TM tape at 2-second intervals. The data were scaled and converted to steering commands without exercising the AGC logic. In this simulation, the CDU for the roll attitude (CDUX) is the same as the CDU computed from the roll command during the flight. The second type of simulation, called a PIPA drive, used the PIPA data from the TM tape as inputs to the AGC. The AGC calculated the roll commands from the PIPA data. Steering commands from both the CDU and the PIPA drives are independent of the environmental trajectory.

5.1 CDU Drive Trajectory

The CDUX (Figure 7) used for the steering commands in the CDU drive trajectory reconstruction were the same as the CDUX recorded on the TM tape during the Apollo 6 entry. This figure which also presents a time history of the AGC roll commands shows the good agreement between the two.

Time histories of the load factor, inertial velocity, and altitude from the CDU drive are compared to the values from the BET in Figures 8 through 10. These parameters are in exceptionally good agreement considering the difference in generation. The altitude deviation of the CDU drive from the BET is presented to better illustrate the two altitude time histories because an altitude profile would show no differences. Figure 8 shows the altitude of the BET minus the altitude of the CDU drive trajectory. After a g. e. t. of 9 hours 42 minutes 30 seconds, the CDU drive altitude is greater than the BET altitude and this deviation reaches a maximum of 7,600 feet. From approximately 9 hours 43 minutes g. e. t. until near the end of the flight, the CDU drive velocity is greater than the BET velocity (Figure 9). This difference in velocity reaches a peak of 600 feet per second at approximately 9 hours 45 minutes 30 seconds which is near the peak altitude of the skip. The peak load factor for the CDU drive was 4.60 g, the second peak was 1.94 g, and the third peak was 1.97 g (Figure 10).

The CDU drive trajectory touchdown point is at 157° 18.0'W and 27° 47.58'N, or 38.5 nautical miles from the CM pickup point and 9.8 nautical miles north of the ground trace.

5.2 PIPA Drive Trajectory

For the PIPA drive simulations, the AGC entry state vector was the actual CM entry state vector recorded on the TM tape and the PIPA data input to the AGC at 2-second intervals was from the TM tape. The roll commands generated in this simulation are almost identical to the roll

commands computed from TM tape data (Figure 4). In Figure 8, the deviation of the PIPA drive altitude from the BET altitude is presented along with the same deviation for the CDU drive. The maximum deviation for the PIPA drive is 3,750 feet occurring at a g.e.t. of approximately 9 hours 44 minutes 30 seconds. The inertial velocity for the PIPA drive is presented in Figure 9 at the points where it differs enough from the BET velocity to be plotted. As can be seen, the PIPA drive velocity deviates less from the BET velocity than that of the CDU drive trajectory. Load factors from the PIPA drive are presented in Figure 10 along with the BET and CDU drive load factors. The peak load factor was 4.677 g, the second peak was 1.903 g, and the third peak was 1.992 g. Time histories of the load factors from the PIPA drive and load factors computed from TM PIPA data are presented in Figure11.

The environment PIPA drive simulation touchdown point was 157° 57.12'W and 28° 0.29'N, which is 22.5 nautical miles from the CM pickup point. This point is 2.8 nautical miles downrange of the pickup point and 22.3 nautical miles north of the ground trace. The CDU drive touchdown point is 34.7 nautical miles downrange and 12.7 nautical miles less in lateral range than the PIPA drive. These two touchdown points are separated by 37.0 nautical miles.

The CM was picked up at 158° 0'W and 27° 38'N. Rescue 6 aircraft estimated the touchdown point to be 157° 59'W and 27° 40'N. Figure 5 illustrates the touchdown points mentioned above and the planned target point.

6. CONCLUSIONS

Evaluation of the operation of the AGC indicates that it performed properly throughout the entry phase. The AGC transferred into the different phases of the guidance equations at the proper times, correctly computed quantities which were recorded on the TM tape, and guided the CM to the vicinity of the target point. A known software problem in the programming of the guidance equations which computed a reference trajectory for the remaining flight caused the CM to miss the target point. Due to this problem, the range in the Upcontrol phase was depressed and the AGC could not fully compensate for this loss. In the Final phase, the AGC maintained a lift vector up orientation, except for 15.2 degree deviations to control predicted lateral range errors, in an attempt to make up the range lost in the Upcontrol phase. However, for the existing conditions, the CM did not have sufficient aerodynamic capability to reach the target point.

Reconstruction of the actual environment trajectory using the TM tape data is a tedious task. The L/D's computed from the PIPA data seem to have a tolerance of about 0.02, and this necessitates many simulations to select the proper L/D. The touchdown points were found to be extremely sensitive to the L/D and indicate that the aerodynamics must be known with a great deal of certainty if the actual touchdown point is to be matched. Vehicle attitude can have a great effect upon the touchdown point and attitude data should be available for comparison, or to control the vehicle. The deadband accuracy for control of the roll angle was found to have great effects on the touchdown point. The deadband value is ±4 degrees, and by forcing the CM to fly on the low side of this deadband, the resulting touchdown point was 512 nautical miles past the CM pickup point. The same commanded roll angles, with the deadband forced to the high side, gave a touchdown point 39 nautical miles short of the CM pickup point. This significant difference in the touchdown points indicates the need for attitude angles.

For Apollo 6, the TM tape data were good and there were no data dropouts in the entry phase. The nature of this flight made it, possibly, easier to reconstruct. The number of different roll commands was relatively small and the lift vector was in the up position for all of the Final phase.

Table I. Entry State Vectors

	Environment	AGC	Initial Tracking Data	Preflight No 2nd SPS
Ground Elapsed Time (hr:min:sec)	9:38:26.56	9:38:26.56	9:38:27.44	9:30:52.386
Inertial Velocity (ft/sec)	32,829.32	32,836.566	32,827.903	32,814.616
Inertial Flight-Path Angle (deg below local horizontal)	5.863	5.8907	5.83798	5.9957
Inertial Azimuth (deg)	89.926	89.8636	89.8989	85.0312
Longitude (deg:min East)	166:14.94	166:12.36	166:16.247	159:18.582
Geodetic Latitude (deg:min North)	32:44.04	32:43.93	32:43.839	32:18.102
Altitude (ft)	401,400	392,512	400,000	399,813

Table II. Trim Aerodynamics

Mach	Trim Angle-of-Attack (deg)	C_L	C_D	L/D
		Postflight		
0.7	155.87	0.3705	0.9442	0.392
1.2	145.03	0.6694	1.044	0.641
2.0	151.84	0.5518	1.267	0.435
3.0	152.56	0.5056	1.213	0.416
5.0	152.2	0.4706	1.134	0.415
8.0	153.0	0.4657	1.150	0.405
10.5	153.25	0.4632	1.158	0.400
13.5	154.2	0.4543	1.180	0.385
18.2	154.2	0.4543	1.180	0.385
21.5	155.00	0.4474	1.193	0.375
31.0	156.7	0.4321	1.224	0.350
		Preflight		
0.7	155.87	0.3705	0.9442	0.392
0.9	150.09	0.4623	0.9913	0.466
1.1	146.38	0.6488	1.068	0.607
1.2	145.03	0.6694	1.044	0.641
1.35	153.04	0.6203	1.270	0.488
1.65	152.35	0.5722	1.280	0.446
2.0	151.84	0.5518	1.267	0.435
2.4	152.11	0.5263	1.259	0.417
3.0	152.56	0.5056	1.213	0.416
4.0	153.20	0.4736	1.166	0.406
6 & above	157.19	0.4265	1.242	0.343

Table III. Comparisons of Roll Commands from TM Tape and from PIPA Drive

Ground Elapsed Time (hr:min:sec)	TM Tape Roll Command (deg)	PIPA Drive Roll Command (deg)
9:38:26.56	15.203	15.203
9:40:16.56	76.232	81.792
18.56	108.510	109.093
20.56	126.612	127.295
22.56	135.298	136.046
24.56	131.198	131.846
26.56	123.969	124.498
28.56	119.265	119.714
30.56	114.568	114.963
32.56	111.421	111.772
9:40:34.56	108.887	109.202
9:40:56.56	92.158	92.296
58.56	91.238	91.367
0.56	-90.430	-90.550
2.56	-84.733	-85.856
4.56	-76.234	-77.297
6.56	-67.344	-68.313
8.56	-54.954	-55.784
10.56	-47.775	-47.832
9:40:12.56	-46.908	-46.937
9:43:54.56	0.0	0.0
9:45:22.56	0.0	15.203
9:45:38.56	15.203	15.203
9:46:40.56	0.0	15.203

Table IV. Velocity and Range to the Target at Entrance into the Guidance Logic Phases

	Entry		Initial Roll		Huntest and Upcontrol	
Ground Elapsed Time (hr:min:sec)	9:38:26.56		9:39:06.56		9:39:58.56	
	Apollo AGC	Simulated AGC	Apollo AGC	Simulated AGC	Apollo AGC	Simulated AGC
Inertial Velocity (ft/sec)	32,836.6	32,836.6	32,935.6	32,935.0	30,398.3	30,401.3
Inertial Range-to-Target (n mi)	2,049.5	2,045.1	1,832.5	1,832.5	1,553.5	1,553.6
Predicted Crossrange Miss (n mi)	-40.0	-39.8	-38.6	-39.8	-12.9	-25.4
	Kepler		Final Phase		Guidance Termination	
Ground Elapsed Time (hr:min:sec)	9:42:18.56		9:43:54.56		9:50:10	
	Apollo AGC	Simulated AGC	Apollo AGC	Simulated AGC	Apollo AGC	Simulated AGC
Inertial Velocity (ft/sec)	21,781.5	21,792.8	19,769.0	19,785.2	2,133.6	2176.0
Inertial Range-to-Target (n mi)	983.1	983.0	658.5	658.2	40.9	39.3
Predicted Crossrange Miss (n mi)	7.1	13.9	-2.6	-5.5	-0.9	-6.7

Table V. Comparison of AGC State Vectors from TM Tape and PIPA Drive Simulation (Units in feet and feet/second)

Ground Elapsed Time (hr:min:sec)		TM Tape	Simulated AGC	Difference TM Tape - Simulated AGC
9:38:24.56	X	18879927	18879926	1
	Y	301653	301653	0
	Z	9851715	9851715	0
	$\dot{X}$	-18103.15	-18103.15	0
	$\dot{Y}$	615.96	615.95	0.01
	$\dot{Z}$	27388.62	27388.61	0.01
9:41:56.56	X	17132602	17132678	-76
	Y	352809	352916	-103
	Z	12282707	12282839	-132
	$\dot{X}$	-18239.44	-18239.09	-0.35
	$\dot{Y}$	301.83	305.76	-3.93
	$\dot{Z}$	24316.44	24320.36	-3.92
9:42:16.56	X	14911894	14911795	99
	Y	282905	284240	-3335
	Z	14938371	14939700	-1329
	$\dot{X}$	-15302.02	-15304.75	2.73
	$\dot{Y}$	-334.92	-320.88	-14.04
	$\dot{Z}$	15497.50	15510.85	-13.35
9:43:52.56	X	13431215	13430774	441
	Y	273413	276441	-3028
	Z	16273431	16276359	-2928
	$\dot{X}$	-15463.11	-15467.52	4.41
	$\dot{Y}$	129.99	151.17	-21.18
	$\dot{Z}$	12316.28	12336.37	-20.09
9:47:00.56	X	11003035	11001522	1513
	Y	265340	273543	-8203
	Z	17933508	17941500	-7992
	$\dot{X}$	-9301.60	-9308.37	6.77
	$\dot{Y}$	-404.99	-371.43	-33.56
	$\dot{Z}$	5285.29	5319.45	-34.16
9:50:08.56	X	10024504	10021680	2824
	Y	183007	199366	-16359
	Z	18387419	18403412	-15993
	$\dot{X}$	-2083.78	-2096.72	12.96
	$\dot{Y}$	-426.18	-368.68	-57.50
	$\dot{Z}$	394.92	450.34	-55.42

Table VI. Touchdown Dispersion Due to IMU Errors

Error Source	IMU Platform Axis	Ratio of Determined IMU Errors to 3σ Values	Touchdown Dispersions in Topocentric Coordinate System at Touchdown (n mi)		
			X Axis	Y Axis	Z Axis
Accelerometer Bias	X	-0.159	0.208	0.008	0.0
	Y	-0.410	0.005	0.542	0.0
	Z	-0.142	0.006	0.057	0.0
Accelerometer Scale Factor	X	-1.23	-0.590	-1.29	0.0
	Y	-0.165	0.017	0.74	0.0
	Z	0.033	0.024	-0.061	0.003
Gyro Drift Rate	X	0.067	0.018	1.26	0.011
	Y	-0.009	0.031	0.0	-0.244
	Z	-0.018	-0.019	-0.450	0.0

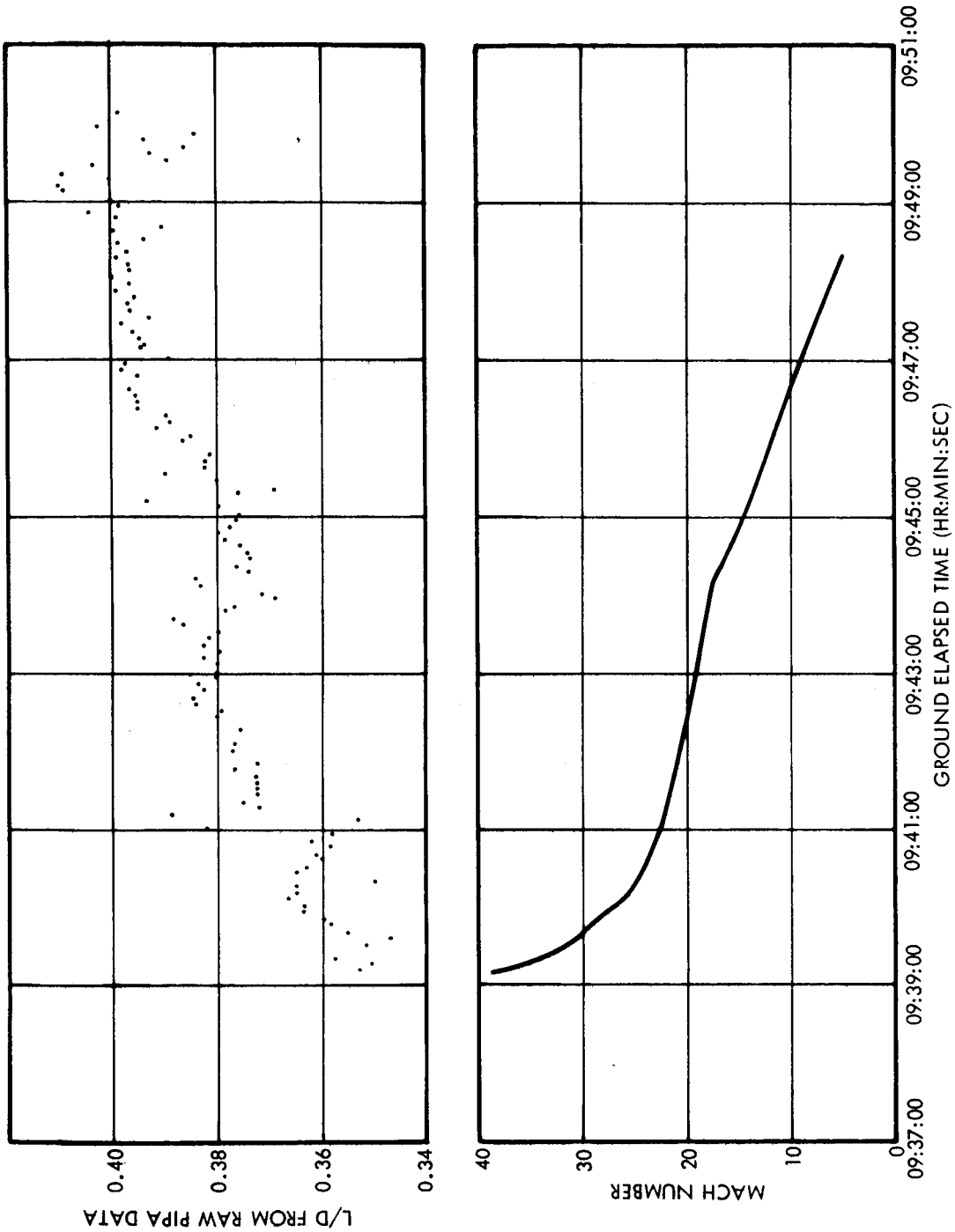

Figure 1. Postflight Aerodynamic Data

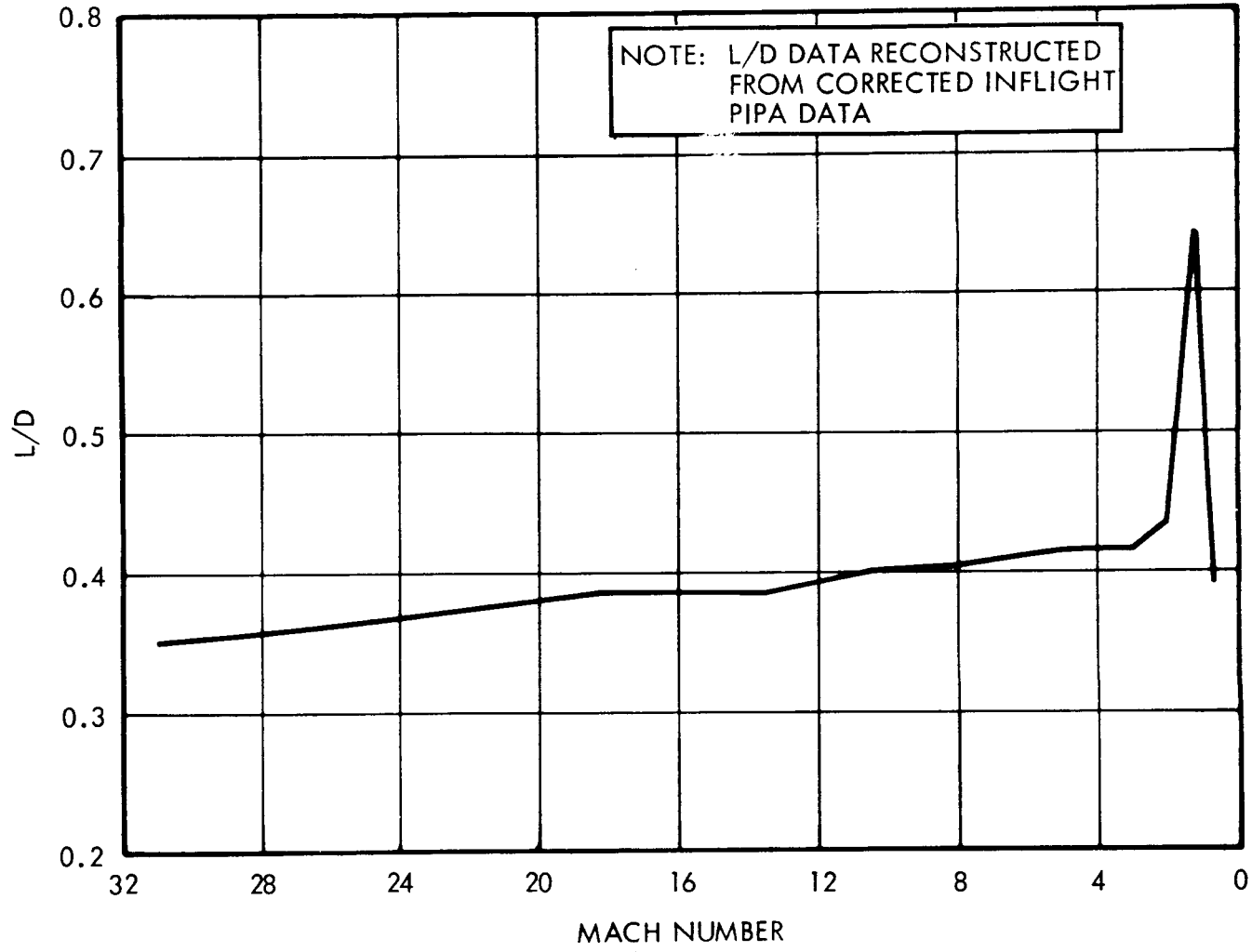

Figure 2. Postflight Lift-To-Drag Ratio

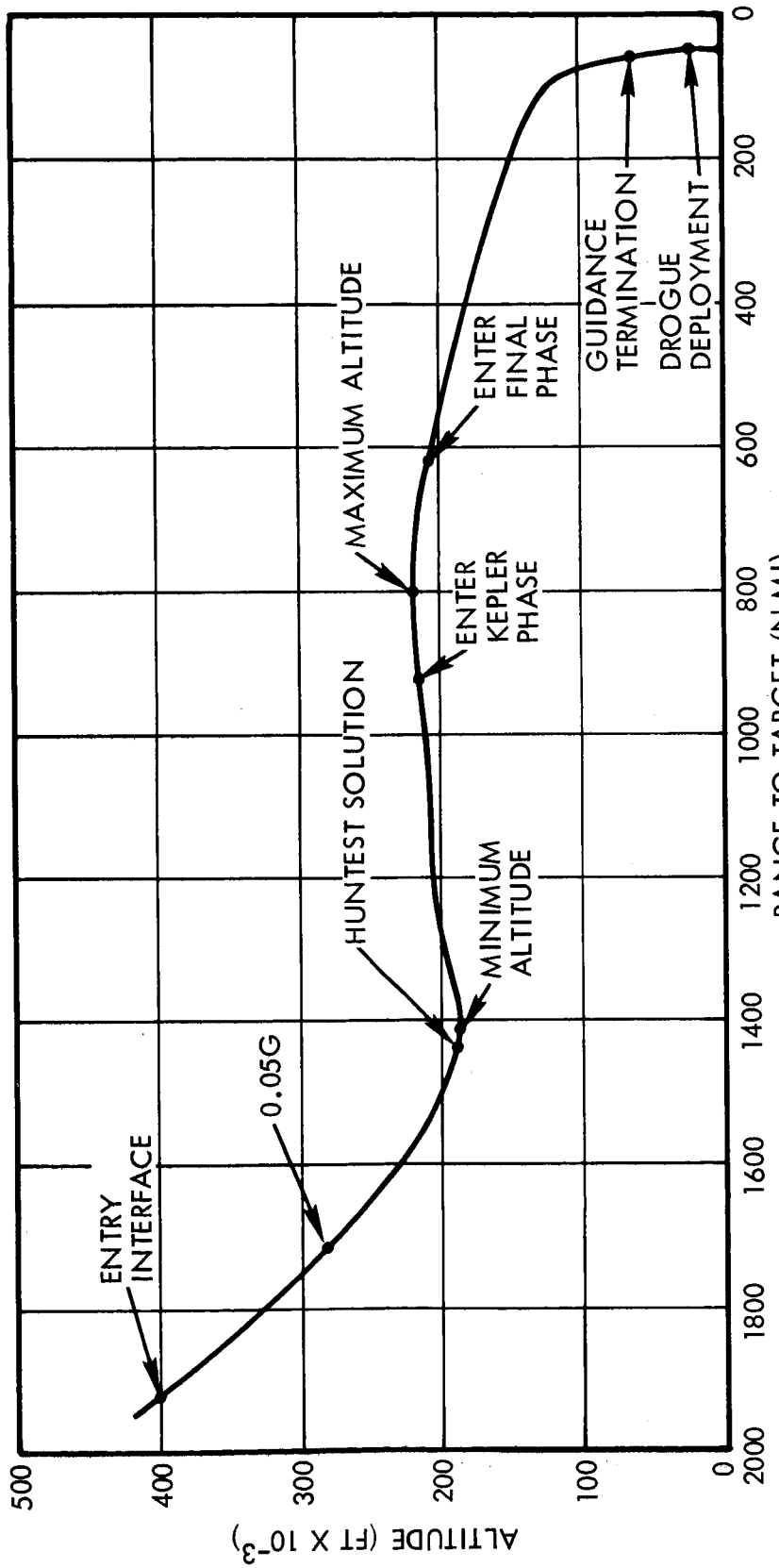

Figure 3. Guidance Phases

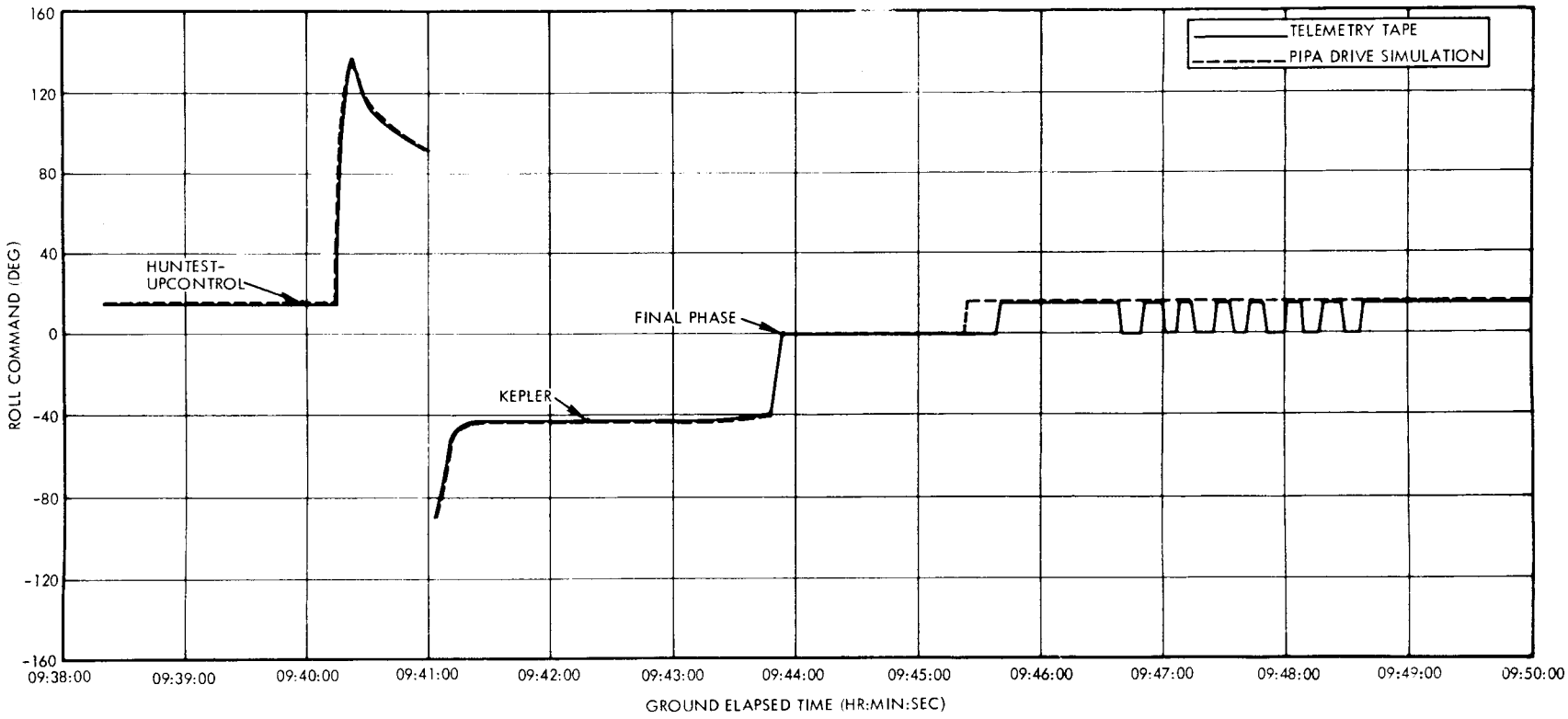

Figure 4. Time Histories of Roll Commands from Telemetry Data and from PIPA Drive Simulation

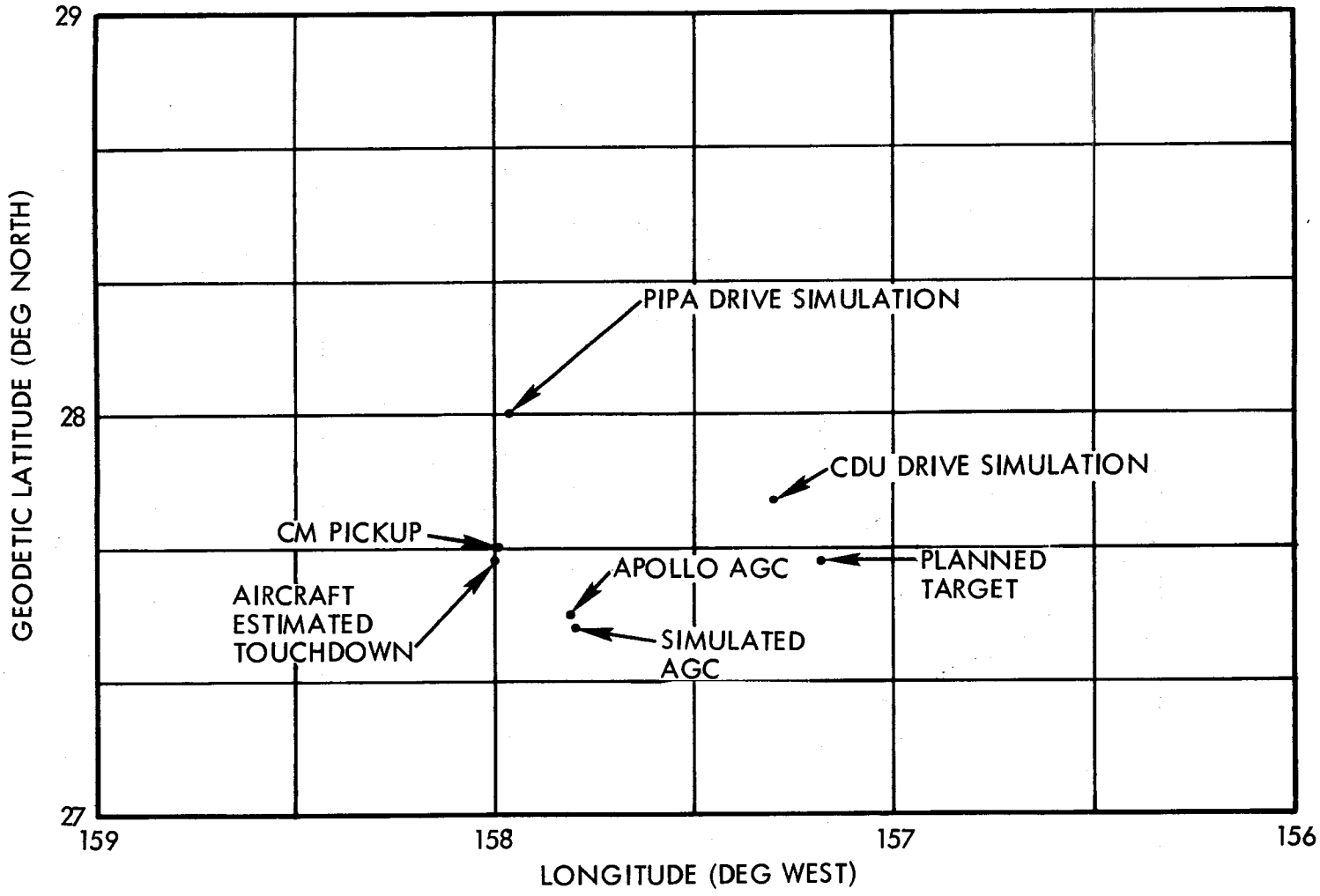

Figure 5. Touchdown Points and Target Location

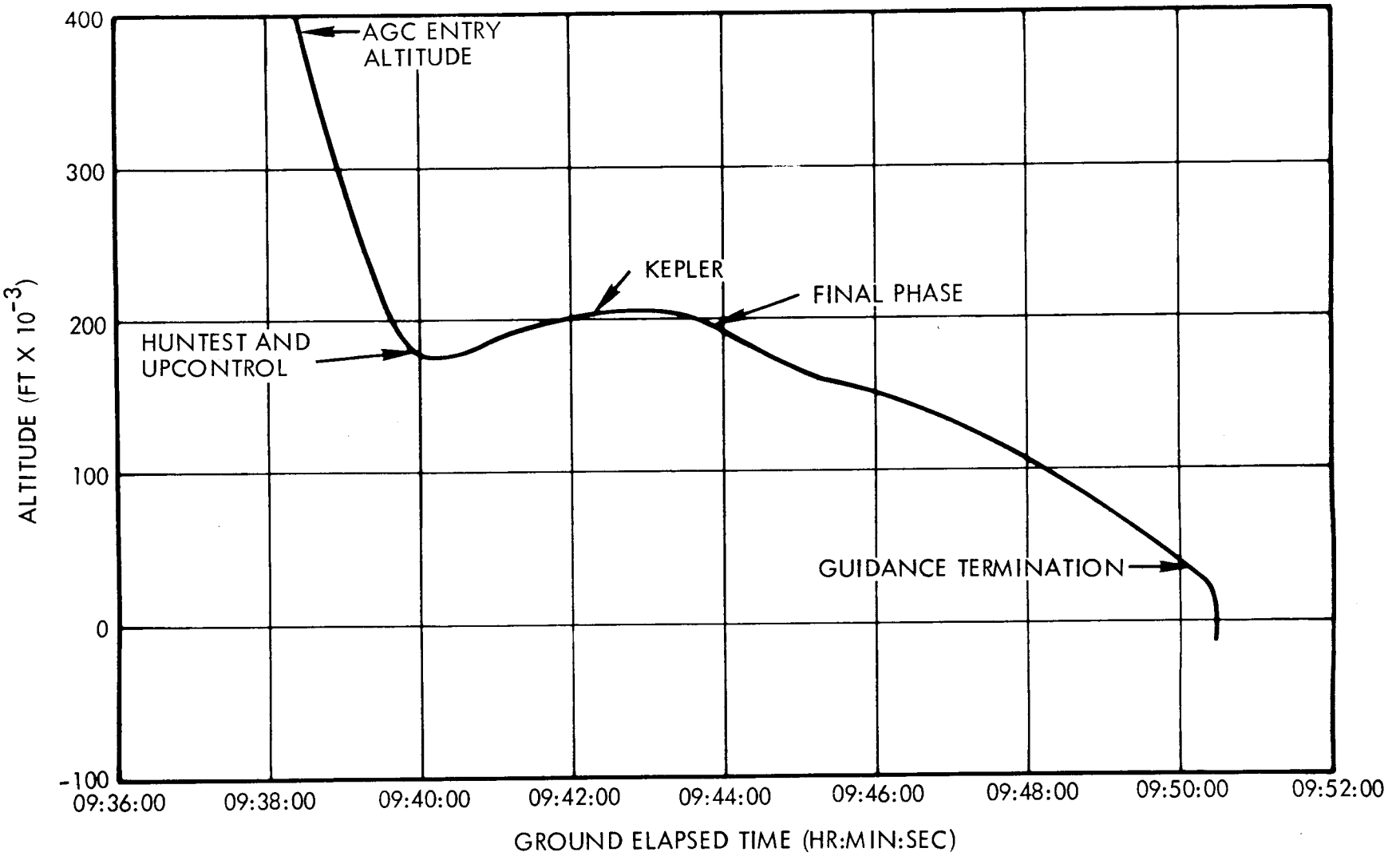

Figure 6. Time History of CM Altitude from Telemetry Data with Guidance Phases Depicted

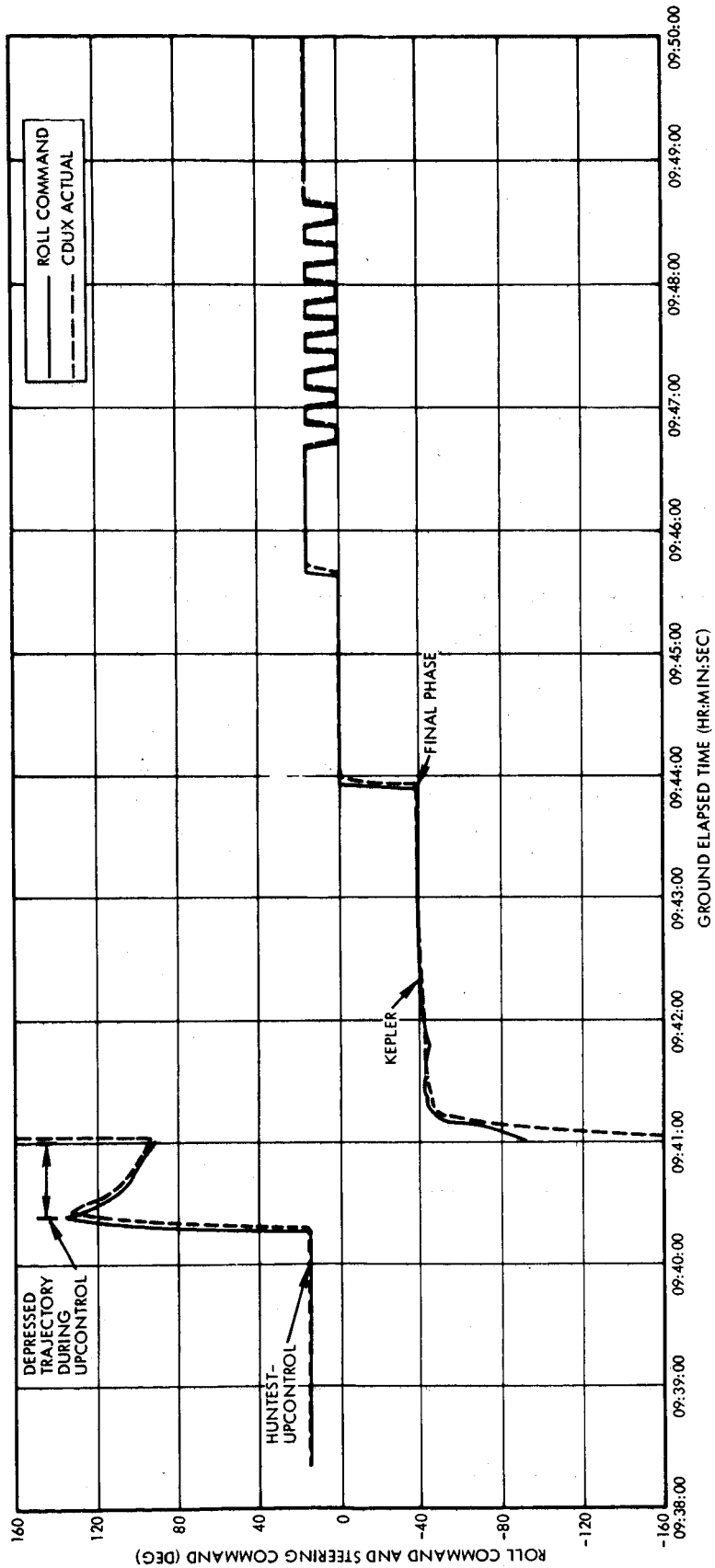

Figure 7. Roll Command and Steering Command from Telemetry Data

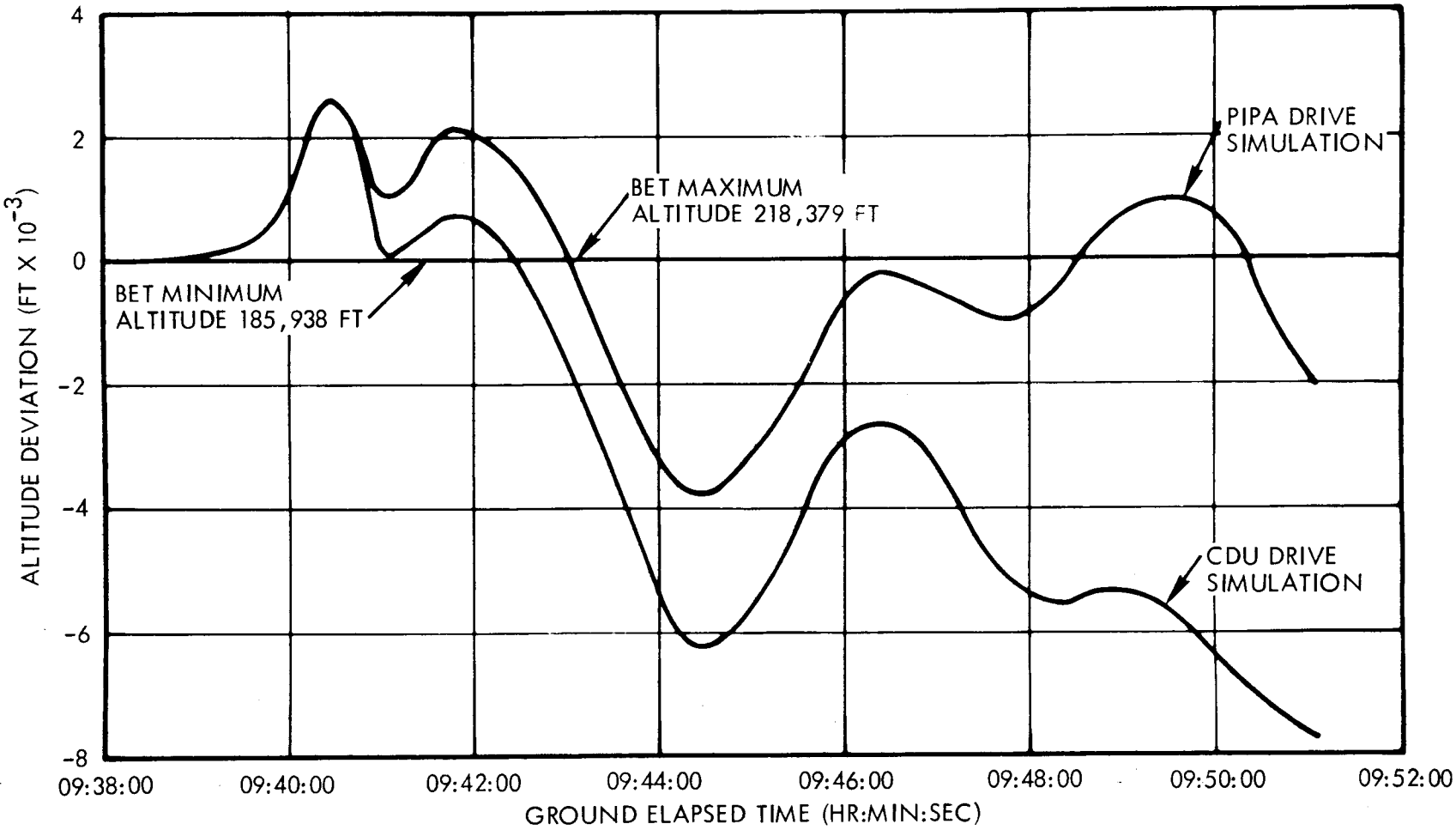

Figure 8. Altitude Deviations of External Drive Trajectories from the BET

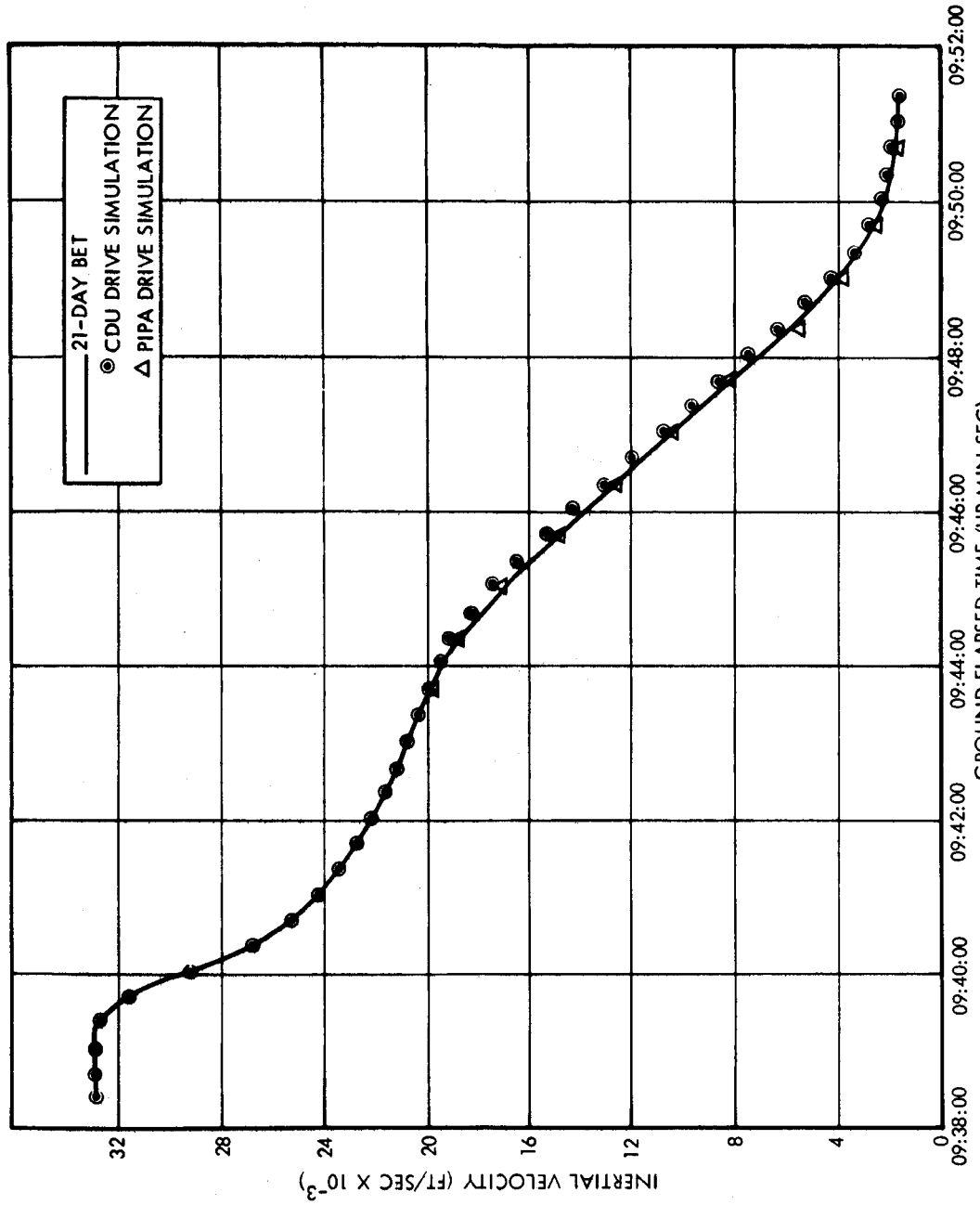

Figure 9. Inertial Velocity Time History Comparisons

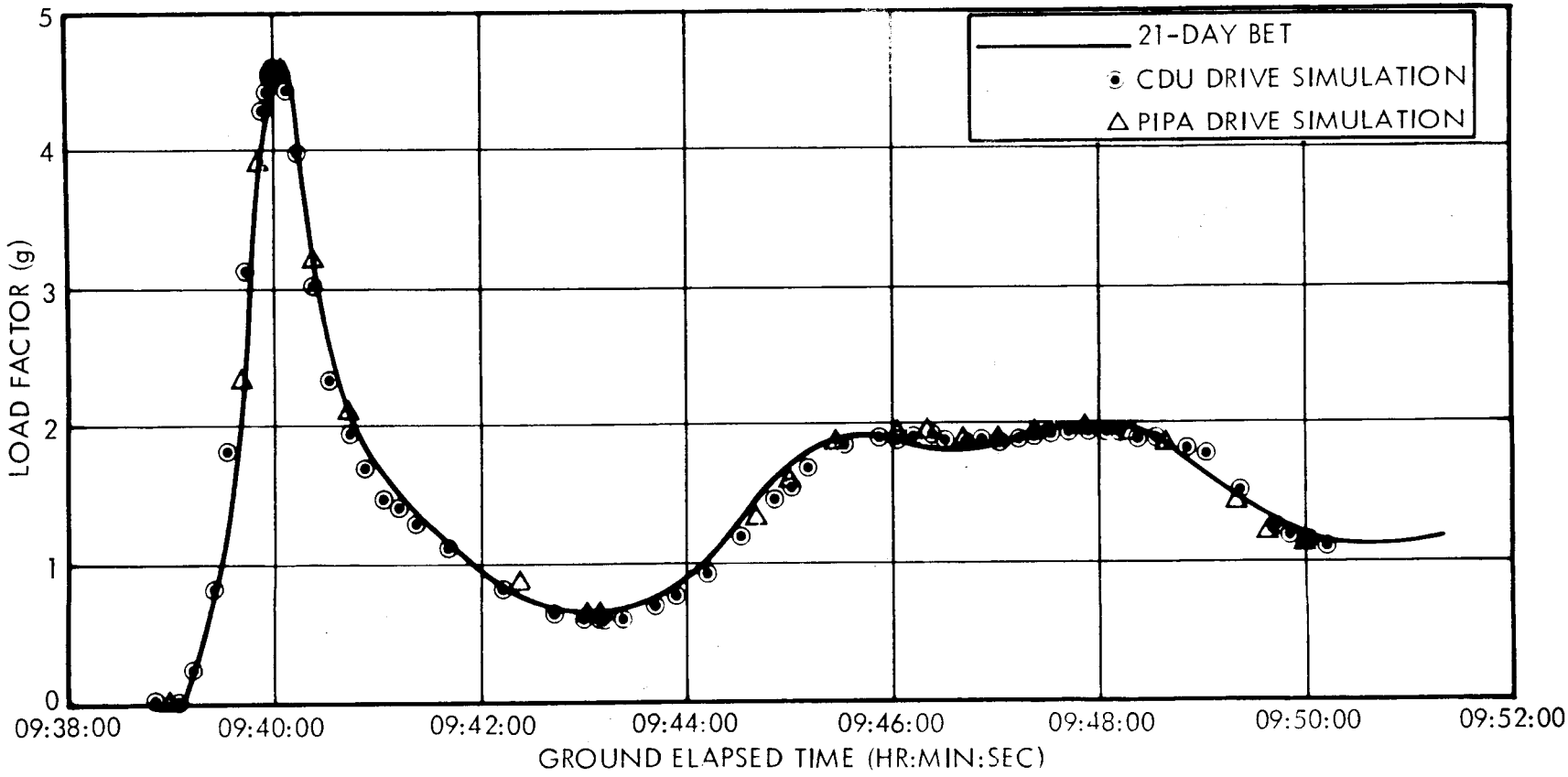

Figure 10. Load Factor Time History Comparisons

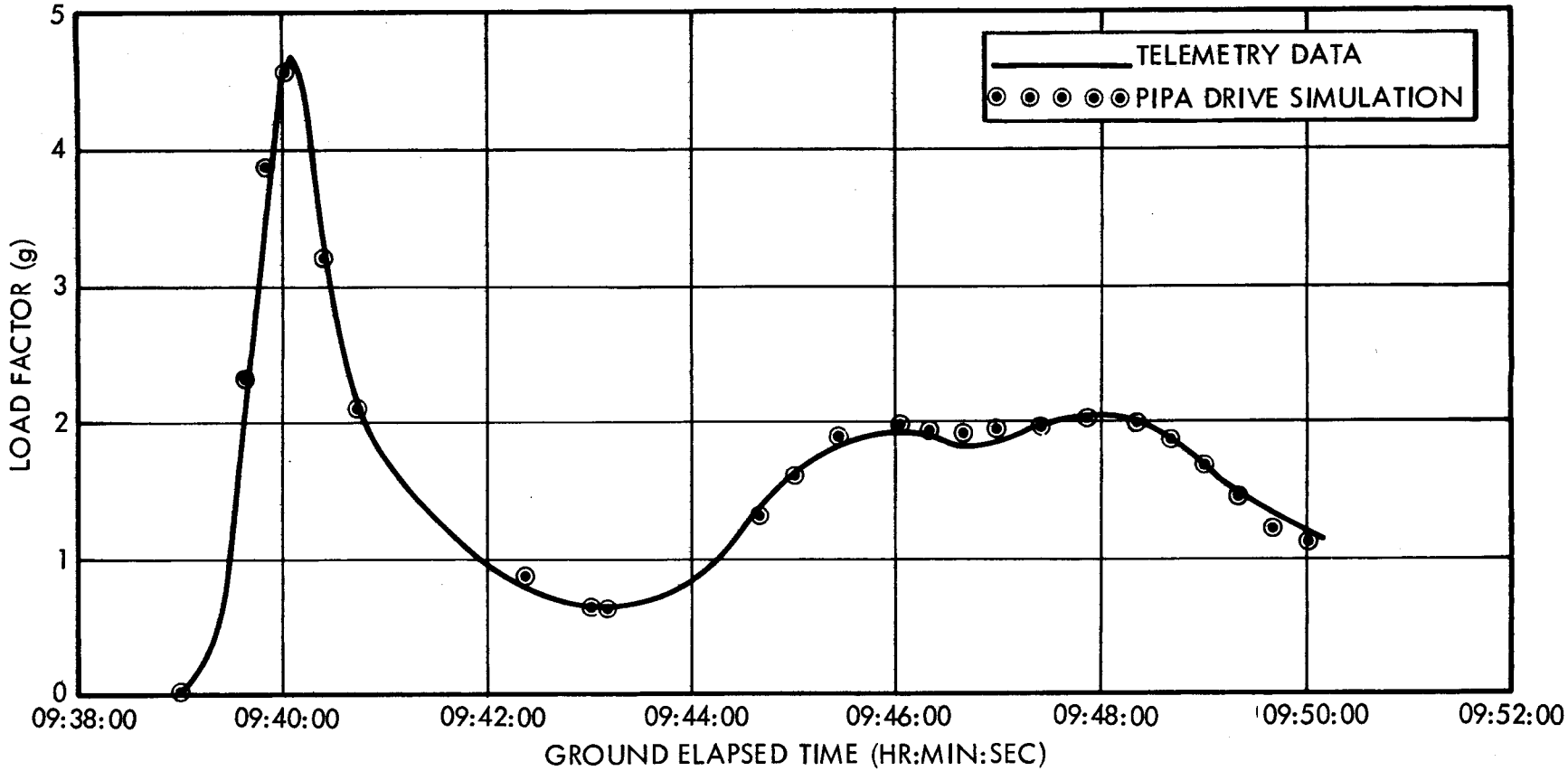

Figure 11. Load Factor Time History Comparisons from Telemetry Data and from PIPA Drive Simulation

REFERENCES

1. Task Agreement for Reentry Support for AS-501/017, AS-502/020, AS-500/104 (High Ellipse Aborts) and AS-500/105 Mission Planning. Task MSC/TRW A-152, October 2, 1967.

2. Entry Flight Data for Mission AS-202. MIT E-2031, October 1966.

3. Hillje, E. R.: Postflight Aerodynamic Data for Inclusion in the MSC Apollo 6 Mission Report. U. S. Government Memorandum ET253/6805-4, May 9, 1968.

4. Atmosphere Entry Ground Support Displays for the Mission Control Center AS-501. MSC Mission Planning and Analysis Division, Internal Note 67-FM-66, May 1, 1967.

5. Kamen, S. A.: Computation of AS-502 Postflight Mass Properties. U. S. Government Memorandum 68-FM74-200, May 1, 1968.

6. Harpold, J. C.: Apollo Entry Targeting Decision. U. S. Government Memorandum 68-FM53-157, April 25, 1968.

7. Reentry Postflight Trajectory Reconstruction and Guidance Evaluation for AS-501 (CSM-017). MSC Internal Note No. 68-FM-90, 05952-H477-R0-00, March 27, 1968.

8. Apollo VI Guidance and Navigation Error Analysis - Final Report. TRW Report No. 05952-H546-R0-00, June 28, 1968.

9. Apollo Missions AS-501 and AS-502 Preliminary Entry Dispersion Analysis (U). TRW Note No. 66-FMT-488, February 2, 1967.